

# Observed Anomaly of Temperature and Mixed Layer Depth Associated with the Madden Julian Oscillation (MJO) Active Phase in the Banda Sea, Indonesia

Nabil<sup>1\*</sup>, Agus Saleh Atmadipoera<sup>2</sup>, Dwiyoga Nugroho<sup>3</sup>, Yuli Naulita<sup>2</sup>, Ariane Koch-Larrouy<sup>4</sup>

<sup>1</sup>Graduate Program in Marine Science, Faculty of Fisheries and Marine Sciences, IPB University

<sup>2</sup>Department of Marine Science and Technology, Faculty of Fisheries and Marine Sciences, IPB University  
Jl. Raya Dramaga, Babakan, Kec. Dramaga, Kabupaten Bogor, Jawa Barat 16680 Indonesia

<sup>3</sup>Oceanographic Research Center, National Research and Innovation Agency

Jl. Pasir Putih Raya No.1, Ancol, Daerah Khusus Ibukota Jakarta 14430 Indonesia

<sup>4</sup>LEGOS, University of Toulouse

14 Av. Edouard Belin, 31400 Toulouse, France

Email: nabil.itk@apps.ipb.ac.id

## Abstract

The eastward propagation of atmospheric waves along the equatorial band from the central equatorial Indian Ocean to the western Pacific Ocean passing through the Indonesian Maritime Continent (IMC), known as the intraseasonal Madden Julian Oscillation (MJO) event, plays an important role on modulating both atmospheric and upper ocean dynamics along its path. This study aims to investigate the MJO active phase dynamics and its impact on changes in near-surface seawater temperature and mixed layer depth (MLD) anomaly in the Banda Sea Indonesia, using multi-datasets of atmospheric reanalysis, satellites derived sea surface temperature (SST), and Argo float between 2017 - 2018. This study revealed that the MJO waves propagate eastward along the southern equator-line over the IMC and pass through the Banda Sea, associated with significant decreased on Outgoing Longwave Radiation (OLR) and increased in zonal wind speed at 850hPa. The study result shows anomalous increased on surface wind speed and SST cooling during of MJO active phase. The amplitude peaks of filtered ocean-atmosphere variables range between 30 - 60 days. Argo float datasets in the Banda Sea for the first time captured upper ocean responses to the arrival of the MJO active phase, as characterized by a negative temperature anomaly of  $\sim 0.3^\circ\text{C}$  in the surface mixed layer, large temperature anomaly of  $\sim 0.8^\circ\text{C}$  in the thermocline layer and the deepening of the MLD of  $\sim 25$  m. Hence, the MJO active phase impacts significantly on surface and vertical temperature cooling and regulate upper ocean mixing intensity in the Banda Sea.

**Keywords:** Intraseasonal Variability, Maritime Continent, Argo float, SST, MJO, MLD

## Introduction

Madden Julian Oscillation (MJO) is a global scale air-sea interaction phenomenon occurs in the equatorial region that dominates in the intraseasonal period (20-100 days) (Jiang et al., 2020). The essential features of MJO active phase are characterized by deep convection, precipitation anomalies and wind anomalies in the entire troposphere. The convective processes occurs in the middle of the equatorial Indian Ocean through Indonesian waters to the western Pacific Ocean with substantial impact to global climate variability, extratropical weather, and subseasonal prediction (Zhang, 2005; Jiang et al., 2020; Lin, 2022). Documentation of MJO study during field campaign and numerical study show that complex air-sea interaction occurs on developing MJO. The suppressed phase is characterized by light wind, reduced surface fluxes, reduced cloudiness, surface

warming, and reduced mixing. The active phase is marked by deep clouds, heavy rainfall, increased westerly wind anomaly, surface cooling, and increased mixing (DeMott et al., 2015).

The SST cooling occurs during MJO active phase period, the study using longterm datasets of OLR as MJO indicator and SST showed high correlation reached 80.2 % in the Indonesian Seas (Baeda et al., 2019). During the MJO propagation across the IMC region, it cause significant sea surface cooling with an area-averaged value of about  $0.35 \pm 0.12^\circ\text{C}$  revealed by SST observation (Balaguru et al., 2021). Observation study using buoy and autonomous profiling float confirmed that drastic cooling of SST ( $2^\circ - 3^\circ\text{C}$ ) was captured during the 2018/2019 austral summer in the Indonesian-Australian Basin and associated by the MJO activities (Feng et al., 2021). The MJO activity also modulates the amplitude of SST diurnal variation in the

Indonesian–Australian Basin observed by Himawari-8 geostationary satellite. The MJO active phase is preceded by strong diurnal SST variations during the MJO suppressed phase. The study concluded that the amplitudes of the SST diurnal variations influenced by surface wind represented by high correlation between those variables (Huang and Feng, 2021). Rapid changes of ocean surface boundary occurred during suppressed and active phase of MJO. During the suppressed phase, the lowest wind speed occurred and modulated latent heat flux and warming the SST resulted on re-stratification on surface layer. The re-stratified upper ocean then prolonged high SSTs by trapping heat near the surface layer until the active phase of the MJO (Hsu *et al.*, 2022). During suppressed phase, the rising temperature trigger marine heat waves (MHW) occurred across Tropical Australia with maximum intensity tended occur in March, consisting with the maximum SST (Benthuisen *et al.*, 2018).

Previous study shows that MJO active phase triggers vertical temperature anomaly in the equatorial region. The study used four years interpolated Argo float data (2003 – 2006) to see changes in the temperature component during MJO active phase. The study reported that there was clear evidence on negative temperature anomalies of surface mixed layer response during the active phase of the MJO. In the deeper layers, the longitude-depth plot from the Indian Ocean to the Pacific Ocean shows the role of the MJO and amplify equatorial kelvin wave on negative temperature anomaly of the water column with the largest amplitude in the thermocline layer (Matthews *et al.*, 2010). The same mechanism of vertical temperature cooling occurs in the northern Indian Ocean – Western Pacific with the largest-amplitude anomalous signals found around the thermocline and extending downward into the deep ocean to below 1000 m (Mao and Wang, 2019). A strong positive MLD anomaly response reached 15 m (peak to peak) during MJO active phase was found using Argo float gridded data in the central part of the Indian Ocean and the western part of the Pacific Ocean. (Drushka *et al.*, 2012). Ocean modeling using Hybrid Coordinate Ocean Model (HYCOM) exhibits a regional maximum of intraseasonal MLD variability reach 14 m of standard deviation with high sensitivity experiments of MJO induced MLD deepening reached 83.7% of the total intraseasonal variability (Liu *et al.*, 2021). Observational study using research vessel in the western coast Sumatra captured significant deepening of MLD reached 45 m during MJO active phase (Moteki *et al.*, 2018). Detail observation study show the surface mixed layer was cooled from above by air–sea fluxes and from below by turbulent mixing observed in the Indian Ocean during MJO active phase (Pujiana *et al.*, 2018).

The Banda Sea has a unique water mass characteristics and being the transformation of two distinct water masses of western and eastern paths of Indonesian Throughflow (ITF). The western path is characterized by fresher and colder originating from Makassar Strait eastward to Flores Sea and the eastern path ITF is characterized by warmer and salty originating from Halmahera Sea and Maluku Sea to Seram. Both water masses mixed in the Banda Sea and going to Indian Ocean through Timor Passage and Ombai Strait. The upper and thermocline layers are influenced by monsoonal characteristics of low salinity water in the Banda Sea originating from Java Sea (Purwandana *et al.*, 2020; Atmadipoera *et al.*, 2022). Based on previous measurement during Indonesian Mixing (INDOMIX) cruise, estimation of Tidal mixing showed the Banda Sea has small dissipation energy lower than Halmahera Sea and outflow straits because the Banda Sea is further away from the tidal generation sites. Hence, The Banda Sea tend to have homogenous water mass characteristics with the similar dissipation value found in the open ocean (Koch-Larrouy *et al.*, 2015; Sprintall *et al.*, 2019). It is consistent with recent study using high resolution of SST which shows low tidal mixing signature in the Banda Sea during normal year and also stronger tidal mixing signatures during the southeast monsoon than in the northwest monsoon (Susanto and Ray, 2022).

Previous studies show strong seasonal variability which controls temperature variation in the surface mixed layer and thermocline layer in the Banda Sea. Using ocean modeling approach, it shows SST variability is influenced by seasonal winds and has a major impact on temperature variations in the Banda Sea (Kida and Richards, 2009). Using EOF approach of long-term SST data, high percentage of seasonal variability was found in the Banda Sea (Habibullah and Tarya, 2021). Observational study investigates seasonal variation of upper-layer water mass using individual CTD Argo float data and reveals seasonal fluctuations of water mass characteristics, MLD and thermocline thickness associated with upwelling (July–September) and downwelling (December–February) period (Atmadipoera *et al.*, 2019). Strong intraseasonal signal is also detected in the Banda Sea. Previous studies have shown that the Banda Sea has a strong SST response to the intraseasonal period. The study revealed that intraseasonal SST variability was strongly influenced by MJO propagation in the Banda Sea which primarily controlled by surface heat flux (Napitu *et al.*, 2015). Recent study showed rapid cooling (14 days) of SST ( $\sim 2^\circ\text{C}$ ) occurs in the boreal winter during MJO active phase episode in the Banda Sea. The 1-D ocean model was used to demonstrate mechanism of vertical mixing induced entrainment cooling contributes more than surface heat flux on SST

cooling (Pei *et al.*, 2021). Previous studies of surface temperature anomaly in the Banda Sea used modeling and satellite observation. However, the vertical temperature characteristics using Argo float observation in the Banda Sea during the MJO active phase is not yet reported. Therefore, the purpose of this study is to describe the propagation of MJO during northwest monsoon, then investigates its impact on temperature and mixed layer depth in the Banda Sea.

## Materials and Methods

The data used in this study are daily atmospheric reanalysis variables, SST, CTD Argo float and the Real-Time Multivariate MJO (RMM) index from 2017 to 2018. Daily atmospheric reanalysis used has  $2.5^{\circ} \times 2.5^{\circ}$  of resolution includes interpolated OLR obtained from NOAA PSL (<https://psl.noaa.gov/data/gridded/data.olrcdr.interp.html>), wind at 850hPa and surface wind obtained from The National Centers for Environmental Prediction (NCEP) / National Center for Atmospheric Research (NCAR) – NOAA (<https://psl.noaa.gov/data/gridded/data.ncep.reanalysis.html>). SST anomaly with  $1/4^{\circ}$  spatial resolution obtained from High-resolution Blended Analysis of Daily SST and Ice – NOAA (Huang *et al.*, 2021) received from <https://psl.noaa.gov/data/gridded/data.noaa.oisst.v2.html>. The CTD Argo float data (ID 6901746) has 2 days of temporal resolution (cycle), 1 m of vertical resolution in the first 300 m and 2 m at the remaining depth with 1000 m of the parking depth. The cycle and vertical resolution of the instrument had been changed at the beginning of the measurement (Atmadipoera *et al.*, 2019). The CTD Argo float data provides information on temperature, salinity, and depth characteristics in the eastern Banda Sea from July 2017–August 2018 obtained from <https://co.ifremer.fr/co-dataSelection/>. RMM index data is obtained from the Bureau of Meteorology (BOM) obtained from <http://www.bom.gov.au/climate/mjo/> which can informatively show the strength of the MJO amplitude off all phases.

The spatial characteristics of the MJO active phase were observed in the equatorial region with longitude  $30^{\circ}\text{E}$ – $150^{\circ}\text{W}$  and latitude  $25^{\circ}\text{N}$ – $25^{\circ}\text{S}$  shown in Figure 1. MJO propagation is depicted through the Hovmöller diagram in the red box extending from longitude  $30^{\circ}\text{E}$ – $150^{\circ}\text{W}$  and averaged on latitude of  $10^{\circ}\text{N}$ – $10^{\circ}\text{S}$ . Time series analysis on ocean-atmosphere variables and mixed layer depth obtained from measurement data focused on the eastern Banda Sea which includes the area recorded by the Argo float ( $129^{\circ}\text{E}$  –  $131^{\circ}\text{E}$ ;  $4^{\circ}\text{S}$  –  $6^{\circ}\text{S}$ ).

The anomaly of variables used in this study is calculated by subtracting the data and monthly climatology in 2017–2018. The anomaly data is filtered using Lanczos Bandpass filter with a 20 – 100 days cutoff period. Following the U.S. Climate Variability and Predictability (CLIVAR) MJO Working Group, using 201 points of points for Lanczos bandpass filter computation got the clear MJO signal (Waliser *et al.*, 2009). The hanning windows of 5 points is applied to the surface wind to get better result of high amplitude during the active phase of the MJO. The spatial composite is constructed by averaging the filtered anomalies during the MJO period for each MJO phase in December 2017 – February 2018. The characteristic and speed of the MJO propagation that passes through the IMC can be analyzed using a Hovmöller diagram. The propagation speed analysis is carried out by identifying the slope formed on the Hovmöller diagram by dividing the longitude and time during the active phase of the MJO (Zhang and Ling, 2017). The MJO propagation speed is separated into three different category includes slow ( $<4 \text{ m.s}^{-1}$ ), moderate ( $4\text{--}5.1 \text{ m.s}^{-1}$ ), and fast ( $>5.1 \text{ m.s}^{-1}$ ) (Chen and Wang, 2020).

Spectrum analysis using the Fast Fourier Transform (FFT) method for bandpass filtered data is carried out to obtain dominant periodicity (Thomson and Emery, 2014). The analysis was carried out on atmospheric and oceanic variables to identify the period in which the peak amplitude at the intraseasonal period within the range of the dominant period of the MJO (30–60 days). Mixed Layer Depth (MLD) from Argo float data is computed to see the MLD anomaly during the active phase of the MJO. The MLD value is determined using the temperature threshold method with finite difference criteria from the reference surface value. The reference surface depth is 10 m to avoid strong diurnal cycles in the surface layer and the temperature threshold is  $0.2^{\circ}\text{C}$  (de Boyer Montégut *et al.*, 2004).

## Result and Discussion

### Propagation of MJO active phase

The MJO active period is determined based on the RMM index in October–December 2017 and January–March 2018 presented in Figure 2. The propagation of the MJO for all location is depicted on the RMM index diagram counterclockwise with strengthening outside the circle. At the end of December 2017 to February 2018, the strong MJO signal propagates from the first to the eighth phase, especially strengthening in the IMC region (phases 4 and 5) in January 2018. The distribution of one MJO cycle has a period of 56 days distributed across all phases with different number of days. This is shown

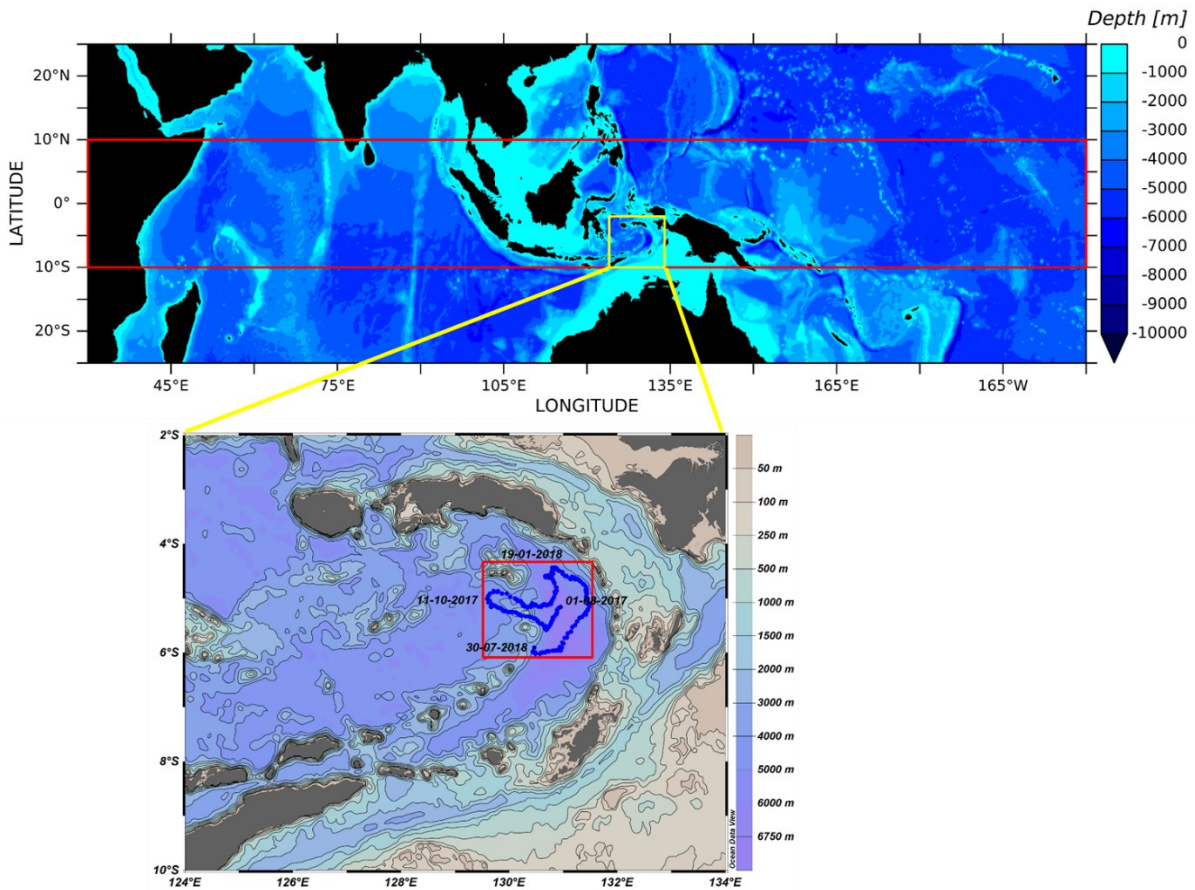


**Figure 1.** MJO propagation analysis using Hovmöller on the red rectangle extends from the Indian Ocean to the Pacific Ocean, time series analysis is conducted the small red rectangle in the Eastern Banda Sea with blue dots showed Argo float trajectory.

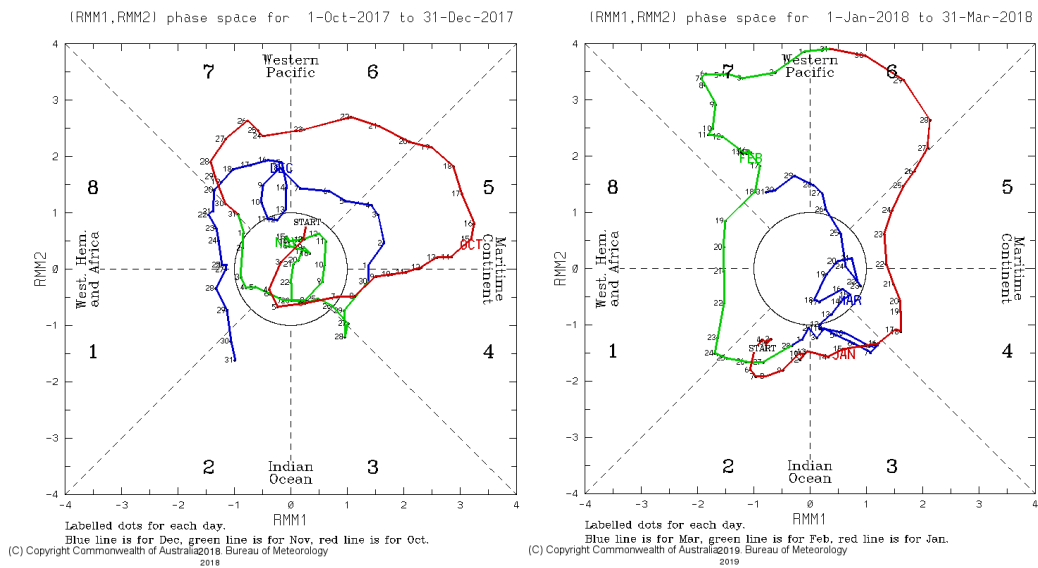


**Figure 2.** Daily RMM Indeks MJO Wheeler-Hendon from October – December 2017 and January – March 2018. The MJO diagram separated into eight different phases or location in anti-clockwise direction, strong active MJO is shown outside the circle (<http://www.bom.gov.au/climate/mjo/>).

in the first phase, the MJO active phase was recorded of 3 days (27 – 29 December), then in the second and third phase the MJO active period in the Indian Ocean reached 18 days (30 December – 16 January). During the fourth and fifth phases, the strong active period of the MJO in the IMC was recorded of 10 days (17 – 26 January). At the sixth and seventh phases (Western Pacific Ocean), the total strong MJO signal recorded were 23 days and 2 days in the eighth phase in the Western Hemisphere. The strength of the MJO amplitude is calculated by squared root of  $RMM1^2 + RMM2^2$  in 2017 to 2018 (Figure 3.) and it shows a significant increase in MJO strength from mid-December 2017 to early March 2018. The high magnitude of the MJO active phase in IMC region was also found on previous study, the result shows the MJO event in January to March 2018 has the strongest amplitude for the last 45 y along the equator and giving strong impact to the extratropical region (Barrett, 2019). Furthermore, based on RMM index amplitude, there are much more active phase compare to weakening phase over IMC and dominantly occur during northwest monsoon (Barrett *et al.*, 2021).

The filtered OLR and U850hPa anomalies is shown in the Hovmöller diagram averaged on  $10^\circ N - 10^\circ S$  (Figure 4.), The strong MJO propagation is occurred at the end of December 2017 to February 2018, shown by the dashed arrow. Based on slope created between longitude and time, the calculated propagation speed of MJO is  $2.74 \text{ m.s}^{-1}$ , categorized as low speed propagation (Chen and Wang, 2020). In the late December to early January 2018, the MJO begins to form in the western part of the Indian Ocean which is characterized by decreasing OLR values ranging from  $5-15 \text{ W.m}^{-2}$  and an increase in 850hPa zonal winds ranging from  $1-4 \text{ m.s}^{-1}$  at longitudes  $30^\circ E - 60^\circ E$ . In January, the strengthening of the MJO was seen stronger than before indicated by decreasing OLR of  $25 - 30 \text{ W.m}^{-2}$  with a zonal wind speed of 850hPa reaching  $4-5 \text{ m.s}^{-1}$  which was seen at longitudes  $60^\circ E - 90^\circ E$ . There is a weakening of the MJO signal in both variables seen when they first entered Indonesian waters (Sumatra Island) at longitude  $100^\circ E$  to longitude  $140^\circ E$  (Papua New Guinea). Then the strengthening occurs after entering the Pacific Ocean at longitude  $150^\circ E$  with negative anomaly values of OLR reaching  $<-30 \text{ W.m}^{-2}$  and U850hPa reaching  $>5 \text{ m.s}^{-1}$ . The MJO active phase along the IMC region shows negative OLR and positive U850hPa characteristics and both propagates dominantly on the southern part equator (Figure 5.). It is shown, the spatial pattern of OLR anomalies during fourth phase, negative OLR anomaly in the Indian Ocean occurs in the southern equatorial of  $10^\circ S$ . During the fifth phase, there is a substantial difference in OLR variation between the southern and

northern equator sides, it captured on the northern equatorial the OLR values are mostly less cloudiness, especially in the Makassar Strait and Sulawesi Sea. The southern propagation also captured from U850hPa variable in the 5th phase with increasing zonal wind in the Indian Ocean equatorial and going towards the southern equator on the IMC, specifically in the Banda Sea.

The propagation of MJO active phase during the northwest monsoon was clearly observed during December 2017–February 2018, especially in January when the MJO passed through the IMC region based on bandpass filtered ocean-atmosphere variables. Spatially, the dominant movement of the active phase of the MJO occurs on the southern side of the equator and strengthens around the Southern Coast of Java, Lesser Sunda Islands, Timor Sea, and Banda Sea. The propagation speed has been calculated by plotted OLR Hovmöller slope and it shows a low speed of  $2.74 \text{ m.s}^{-1}$ , so the MJO active phase episode is longer than the average found previously with a speed of  $\sim 5 \text{ m.s}^{-1}$  (Zhang, 2005). These results are still in accordance with the tabulation of the MJO zonal velocity conducted by Zhang and Ling (2017) which states that from the tabulation of MJO events, the velocity range is between  $2-3 \text{ m.s}^{-1}$ . Recent study also found low velocity and categorized it as low MJO velocity ( $<4 \text{ m.s}^{-1}$ ) (Chen and Wang, 2020).

#### **Timeseries of filtered ocean-atmospheric data**

The time series plot on the OLR, U850hPa, and surface wind speed variables for one year (August 2017 to July 2018) is presented in Figure 7. In general, the anomalies of all variables show appropriate fluctuation during the MJO active phase. This can be seen from the negative OLR anomaly on 19 January 2018 reached  $-34.7 \text{ W.m}^{-2}$ , then followed by an increase in U850hPa reached  $4.06 \text{ m.s}^{-1}$ . The OLR and U850hPa anomalies on late January agree with high amplitude of RMM index at the same time. There is an increase surface wind speed heading to southeast in January–February 2018 with the strongest wind speed reached  $7.54 \text{ m.s}^{-1}$  on 28 January. The active phase MJO episode exhibit SST cooling in the Banda Sea with the lowest value reached  $-0.14^\circ C$  on 23 January 2018. There is a lag for 4 days between SST cooling and MJO active phase (lowest OLR). The results of the amplitude spectrum of the variables plotted in timeseries above are shown in Figure 8. The OLR and U850hPa variables have the highest peak amplitude spectrum values of  $8.792 \text{ W.m}^{-2}$  and  $1.034 \text{ m.s}^{-1}$  with periods of 32.8 days and 53.3 days respectively. The highest amplitude spectrum of the SST spectrum reached  $0.112^\circ C$  with a period of 40.6 days and the second peak has a value of  $0.110^\circ C$  with a period of 56.8 days.

The calculated amplitude spectrum of ocean-atmospheric datasets agrees with previous review

with maximum spectral peak of the MJO activity ranging around 30 to 90 days (Zhang, 2005).

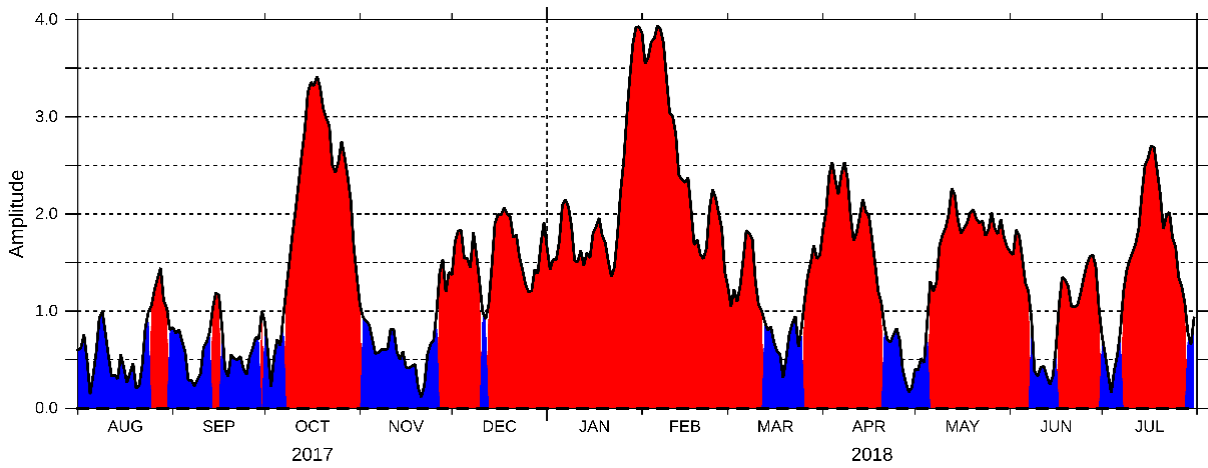


Figure 3. Squared root of  $RMM1^2 + RMM2^2$  in August 2017 to July 2018 (Figure 3), red polygon shows MJO amplitude above one.

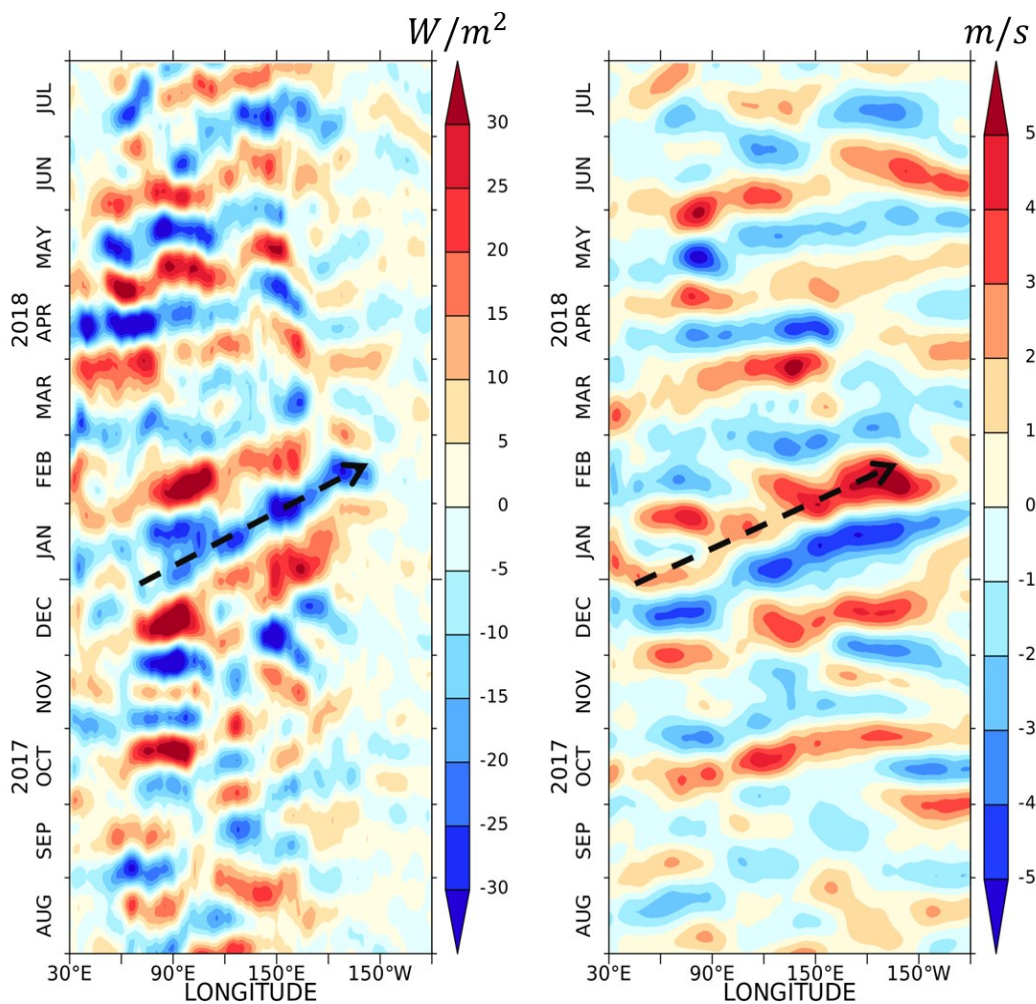
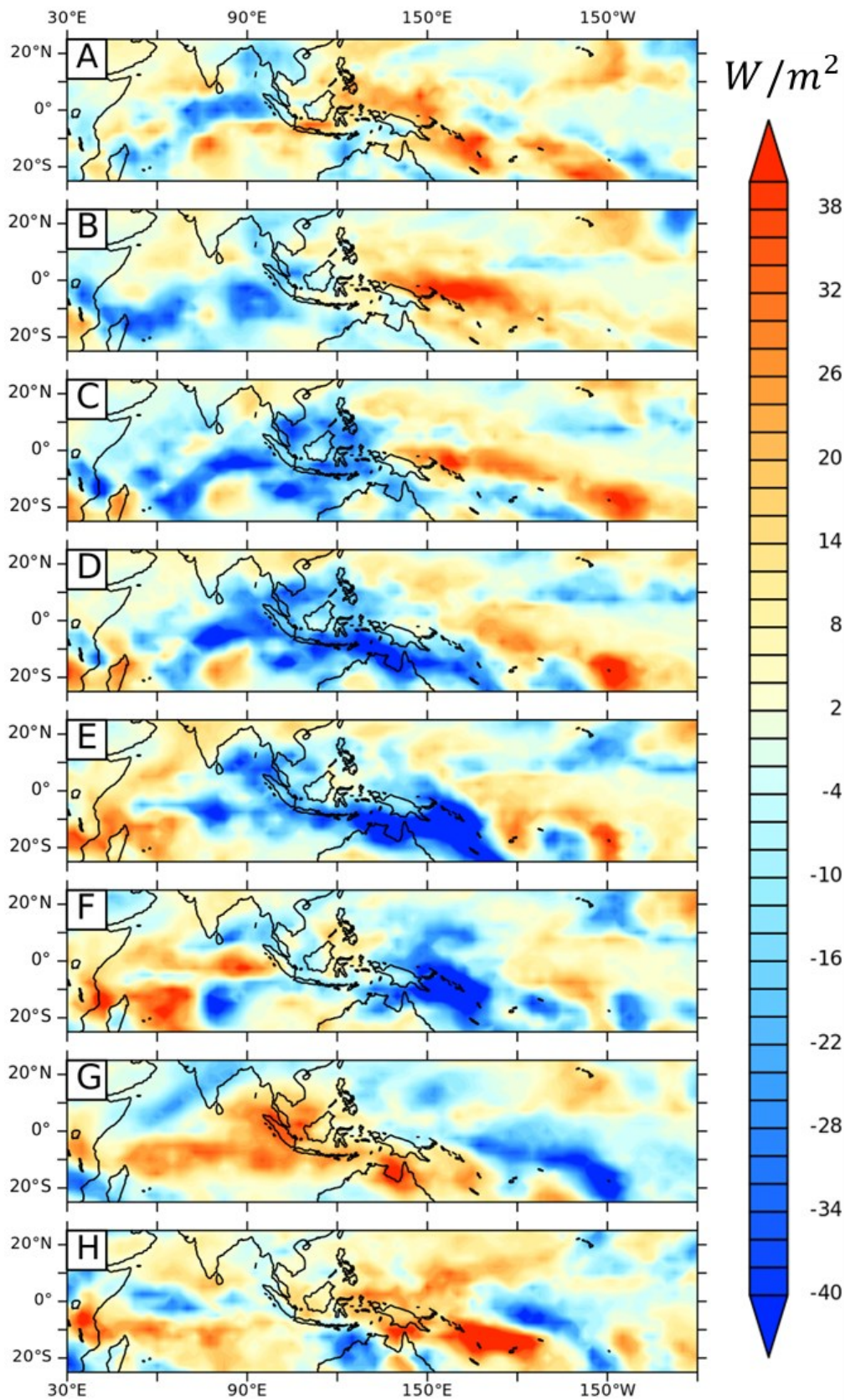
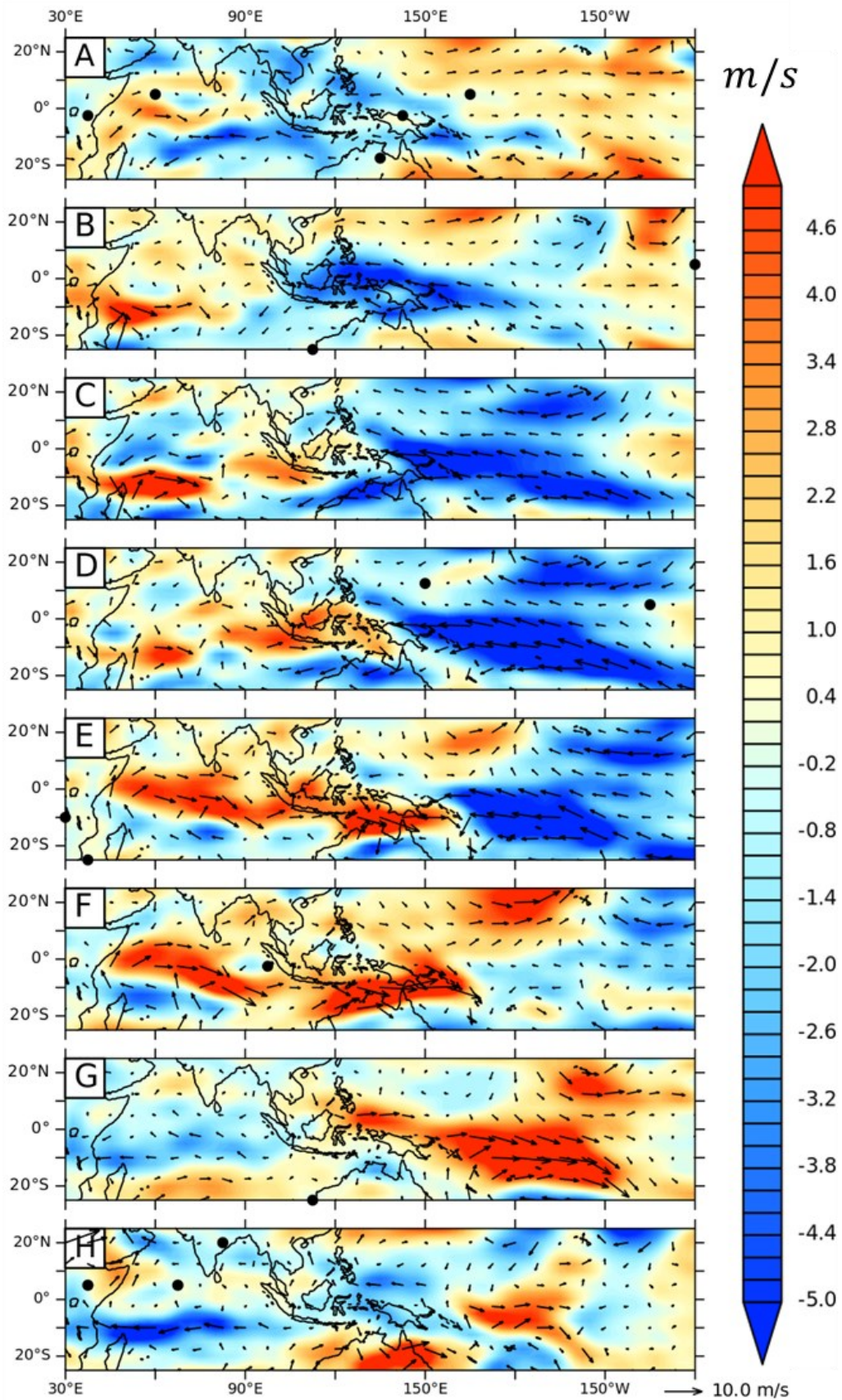


Figure 4. Hovmöller diagram of filtered OLR ( $W \cdot m^{-2}$ ) anomaly (left) and filtered U850hPa ( $m \cdot s^{-1}$ ) anomaly (right) averaged at  $10^{\circ}N - 10^{\circ}S$  in August 2017 - June 2018, dashed arrow indicates MJO active phase episode.



**Figure 5.** MJO propagation is clearly seen by spatial negative anomaly of OLR from Indian Ocean to Pacific Ocean through IMC in the phase 1–8 (A–H).



**Figure 6.** MJO propagation is clearly seen by spatial positive anomaly of U850hPa from Indian Ocean to Pacific Ocean through IMC in the phase 1–8 (A–H).

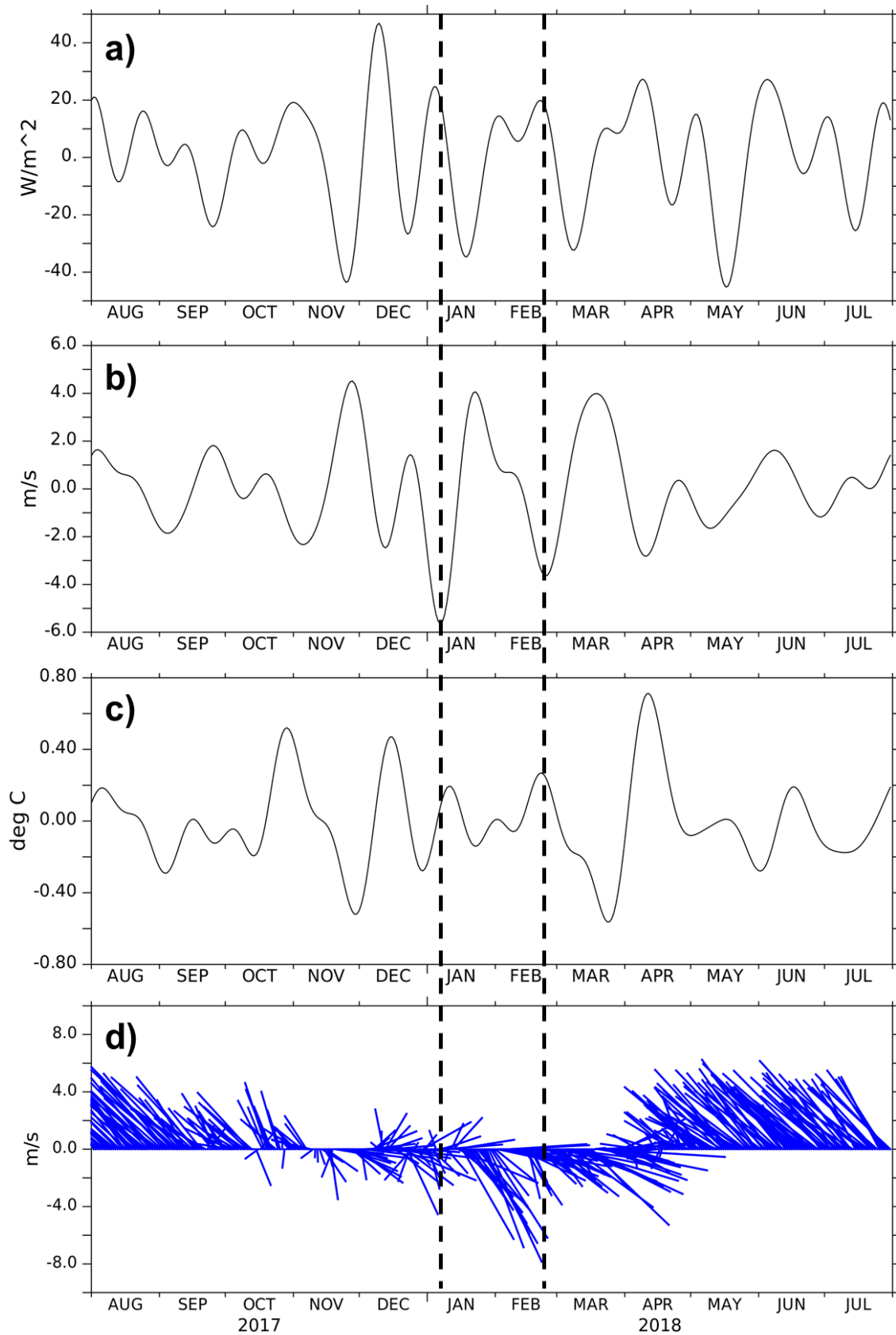


**Figure 7.** Bandpass filtered for time series plot of (a) OLR, (b) U850hPa, (c) SST, and (d) smoothed 10 m surface wind speed, averaged at 129°E-131°E and 4°S-6°S on August 2017 – July 2018.

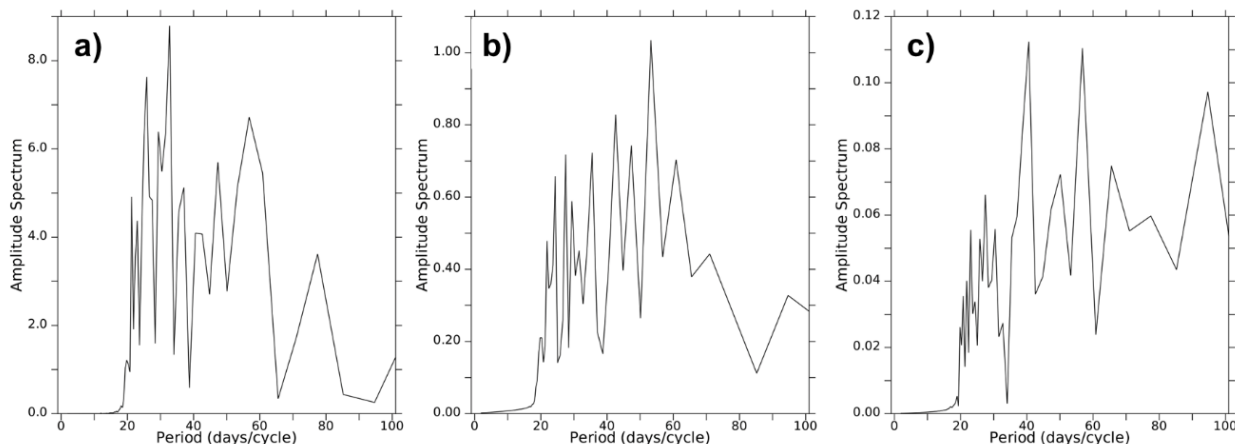


Figure 8. Calculated timeseries amplitude spectrum of (a) OLR, (b) U850hPa, (c) SST.

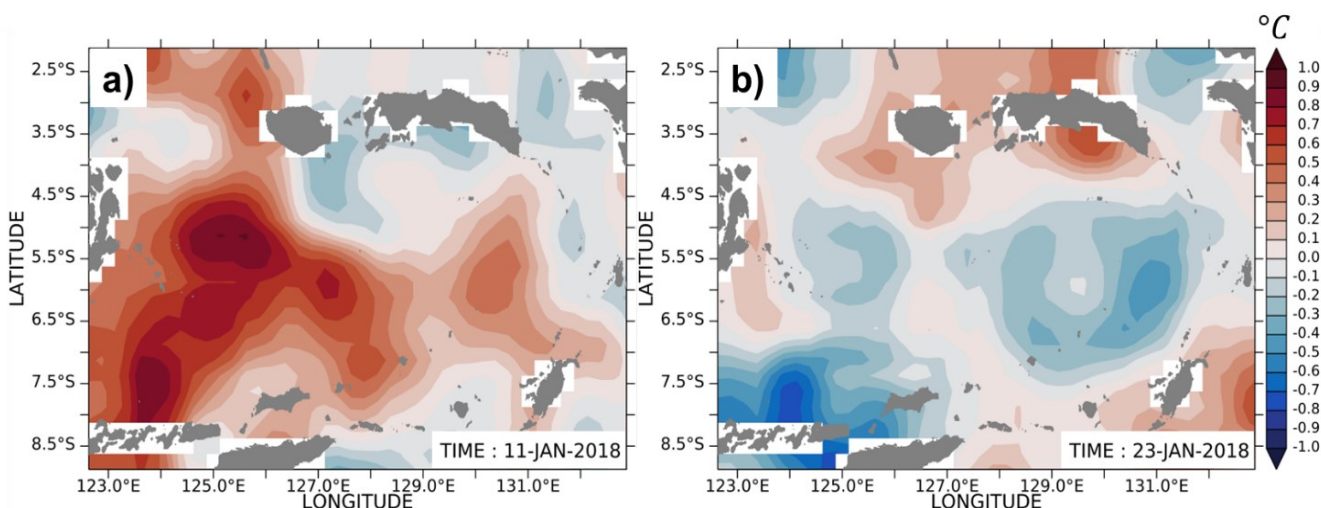


Figure 9. SST anomaly during MJO (a) suppressed phase and (b) active phase

**Temperature and MLD anomaly during MJO active phase**

The difference in surface temperature in the Banda Sea is shown in spatial SST plot during MJO suppressed and active phase MJO (Figure 7.). During the MJO suppressed phase, there is positive anomaly of SST ranging from 0.1°C – 1°C dominates in the Banda Sea. The highest SST anomaly shown on the western part of the Banda Sea reached ~1°C and it tends to be lower on the eastern part of the Banda Sea with the highest SST reached ~0.5°C. The opposite condition is shown during the MJO active phase episode that exhibit SST cooling of 0.1°C – 0.8°C, with the lowest negative anomaly value on the southwest of the Banda Sea reached ~0.8°C and ~0.5°C on the eastern Banda Sea. The lowest response of SST to the active phase of MJO as indicated by the lowest OLR value in the timeseries area was occurring in 4 days.

The negative anomaly of SST spatially reaches -0.8°C and at time series locations it reaches -0.14°C when the active phase of the MJO takes place in the Banda Sea. The drastic SST cooling during MJO active phase also found by Napitu *et al.* (2015) reached ~1°C and widespread in the entire Banda Sea during northwest monsoon 2007, with significant contribution on air-sea heat flux compared to wind stress. However, using sensitivity analysis, Pei *et al.* (2021) found that entrainment cooling produced by wind induced vertical mixing contributes more than surface heat flux for driving the basin-wide SST cooling (~2°C) during the northwest monsoon 2015. We found that the SST cooling associated with higher wind speed and negative OLR anomaly during MJO active period. A lag in the SST cooling response that occurred in the Banda Sea for about 8 days before returning to a positive SST anomaly. This delay was also found by Liang *et al.* (2018) where the SST response to the MJO in the Indian Ocean has a lag of about 5 – 15 days.

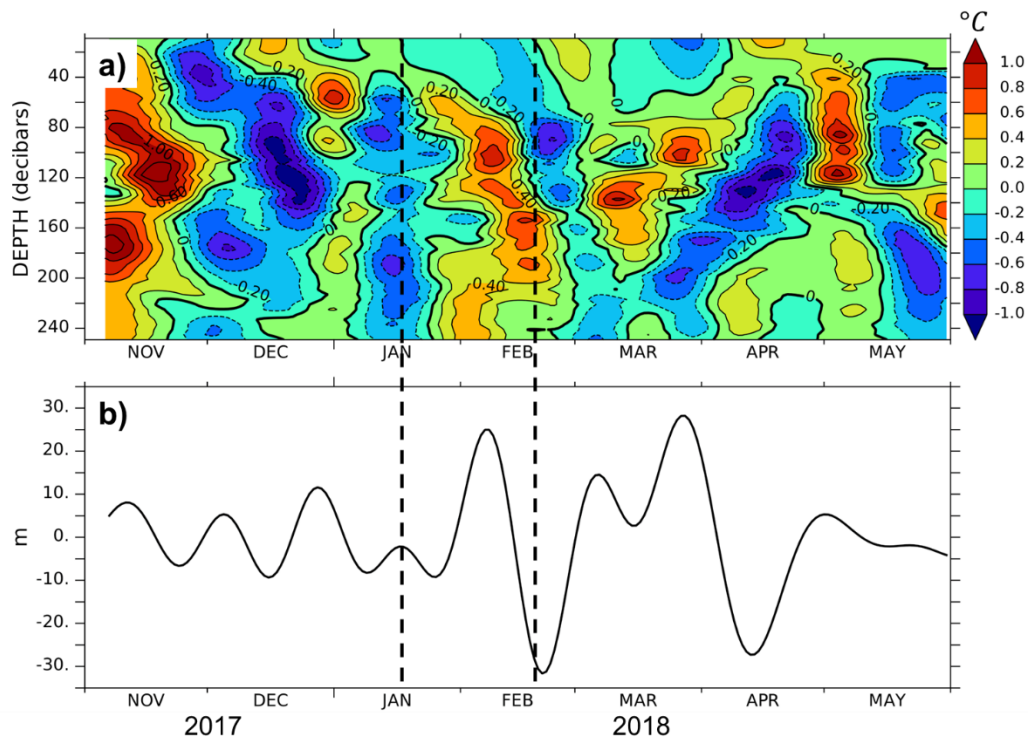


Figure 10. (a) Vertical temperature anomaly ( $^{\circ}\text{C}$ ) observed from Argo float and (b) derived MLD on November 2017 – May 2018

The vertical temperature anomaly of the filtered Argo float at a depth of 0 m to 250 m is presented in Figure 9. In general, the vertical temperature cooling with time from the surface layer to the deeper layer shows a strong response to the active MJO phase. The negative temperature anomaly has a range of  $0.1^{\circ}\text{C} - 1^{\circ}\text{C}$  at a depth of 0 to 250 m from mid-January to February 2018 with the highest negative temperature in the thermocline layer. It is seen that there is a lag of temperature cooling in the surface layer to the deeper layers. This is shown from the results of averaged temperature every 20 m from surface layer to 100 m of depth, with the lowest temperature value of  $-0.29^{\circ}\text{C}$  occurring on February 12. Then at a depth of 40 – 60 m the lowest temperature value is  $-0.27^{\circ}\text{C}$  which occurs on February 17, and at a depth of 80 – 100 m the lowest temperature value is  $-0.75^{\circ}\text{C}$  on February 23. At a depth of 100 – 250 m, the temperature cooling is not as large as the thermocline layer with values ranging from  $0.1^{\circ}\text{C} - 0.6^{\circ}\text{C}$ . In contrast to the passive phase of the MJO that occurred in early January 2018, the positive anomaly value of the MJO was clearly visible in the water column with a value of  $0.1 - 0.8^{\circ}\text{C}$  with the highest positive temperature anomaly also found in the thermocline layer.

The Banda Sea has homogenous water mass structure in the surface layer down to thermocline layer and influenced seasonally by fresh water originating from Java Sea (Atmadipoera *et al.*, 2022)

and it also has a small tidal dissipation energy value similar to open ocean (Koch-Larrouy *et al.*, 2015), hence the Banda Sea has a stable water mass. Consequently, the role of ocean processes on regulating mixing in the upper layer is weaker than atmospheric forcing contributes on mixed layer temperature cooling and deepening of MLD during MJO active phase. The strong response of temperature cooling around  $0.1^{\circ}\text{C} - 0.8^{\circ}\text{C}$  in the water column occurs during the MJO active phase indicated by filtered Argo temperature data in the Banda Sea. Compared with previous study, the result agreed with changes in temperature cooling of  $0.05^{\circ}\text{C} - 0.4^{\circ}\text{C}$  in the surface mixed layer observed by gridded Argo at the equator from the Indian Ocean to the Pacific Ocean averaged on  $1.5^{\circ}\text{N} - 1.5^{\circ}\text{S}$ . In addition, there is strong temperature cooling in the thermocline layer forced by equatorial kelvin waves (Matthews *et al.*, 2010). Our result showed that there is a difference of  $0.2^{\circ}\text{C}$  smaller than the temperature anomaly in the Pacific Ocean. However, we found similar pattern of high temperature amplitude in the thermocline layer compared with surface and deeper layers. Temperature cooling ( $\sim 2 - 3^{\circ}\text{C}$ ) was also found during MJO active phase trough temperature profiling in the Indo-Australia by Feng *et al.* (2021), while the decreasing of temperature in the surface layer from the Argo float temperature ranges  $0.1 - 0.2^{\circ}\text{C}$ . This temperature difference occurred because of the Indo-Australian basin area highly responds to MJO events compared to the Banda Sea which is shown from

larger surface wind speed, with a value of  $10 \text{ m.s}^{-1}$  in the first MJO and reaching  $30 \text{ m.s}^{-1}$  modulated by tropical cyclone activity in the second MJO. Hence, we suggest that there is different cooling impact on intraseasonal period especially in the MJO active phase between open ocean especially on Equatorial Pacific Ocean and Indo-Australia basin compared with Banda Sea in the interior of Indonesian Seas.

The intraseasonal MLD anomaly (Figure 10.) shows strong fluctuations occurring on January to March 2018. The plot shows a positive MLD anomaly reaching 24.97 m on February 8, around 20 days after the active phase of the MJO on January 19 and previously shallowing of the MLD value reaching -9.22 m on January 26. Thus, the difference in MLD during the MJO period reached 34.19 m. The deeper MLD response associate to the strong amplitude of the Wheeler-Hendon index at the same time followed by a decrease in the OLR value and an increase in surface wind speed. Strong MLD fluctuations also shown in March 2018 with a maximum value of 28.21 m on 28 March and the previous minimum value of 2.69 m on 15 March with a difference in MLD value of 25.52 m. Strong MLD response in March corresponds to the low OLR value and the increase in surface winds, while the amplitude on the RMM index shows the MJO in a weak condition.

During the MJO active phase, there is a deepening of MLD reaching  $\sim 25 \text{ m}$  in February 2018, this result agrees with previous study which mentions the MLD deepening of more than 15 m in the Indian Ocean and the Pacific Ocean due to the MJO active phase (Drushka *et al.*, 2012). The response of deepening MLD is presumably triggered by the increasing surface wind speed and intensify surface mixing that occurred at the end of January 2018 along with the MJO active phase episode. The opposite condition was shown during suppressed phase that the shallowing MLD of  $\sim 10 \text{ m}$  occurs in mid-January 2018 when weakened of wind speed occurred. Deepening of MLD occurred during MJO active phase reached 10–50 m was also found by Feng *et al.* (2021), and agree with our result with deepening of MLD reached  $\sim 25 \text{ m}$ . The MLD deepening mechanism is likely due to an increase in wind speed so that colder water below the surface mixed layer was entrained into the surface layer during the MJO that has been proven by Pei *et al.* (2021) through 1-D model. The temperature cooling is also triggered by the convective mixing process during the active phase of MJO and resulted high shear instability (Hsu *et al.*, 2022). Furthermore, The Banda Sea has a strong wind stress, presents the deepest mixed layer with an average of 65 m (Koch-Larrouy *et al.*, 2015). Both contributed to an increase in the deepening of MLD, while warming in surface temperature and weakened wind causes the

shallowing of MLD. Hence, we suggest that increasing surface wind speed induced mixing play an important role on temperature cooling and deepening on MLD during MJO active phase.

## Conclusion

The MJO active phase in January – February 2018 is clearly seen from the low OLR of  $-34.7 \text{ W.m}^{-2}$  which indicates a strong convective process and simultaneously followed by increasing U850hPa of  $4.06 \text{ m.s}^{-1}$ . The amplitude spectrums of OLR and U850hPa variables have highest amplitude spectrum peaks periods of 32.8 days and 53.3 days respectively and agree with MJO dominant period. During the MJO active phase, there is significant increase on surface wind speed reached  $7.54 \text{ m.s}^{-1}$ . Rapid SST cooling of  $0.1^\circ\text{C}$ – $0.8^\circ\text{C}$  during MJO active phase was found in the Banda Sea. Negative temperature anomaly ( $\sim 0.3^\circ\text{C}$ ) occurs in the surface mixed layer with the highest temperature cooling in the thermocline layer ( $\sim 0.8^\circ\text{C}$ ) and followed by deepening of MLD ( $\sim 25 \text{ m}$ ).

## Acknowledgement

The authors wish to acknowledge the use of PyFerret program for analysis and graphics in this paper. PyFerret is a product of NOAA's Pacific Marine Environmental Laboratory (Information is available at <http://ferret.pmel.noaa.gov/Ferret/>). The Banda Indonesian Throughflow Experiment (BIDE) – Argo float research project was partly financed by the Directorate General of Higher Education - Ministry of Education, Culture, Research and Technology of Indonesia under applied research excellent university scheme, contract no.1626/IT3.11/PN/2018 (ASA as a principal investigator). The constructive comments from anonymous reviewers are greatly appreciated.

## References

- Atmadipoera, A.S., Koch-Larrouy, A., Madec, G., Grelet, J., Baurand, F., Jaya, I. & Dadou, I., 2022. Part I: Hydrological properties within the eastern Indonesian throughflow region during the INDOMIX experiment. *Deep. Res. Part I Oceanogr. Res. Pap.* 182: p.103735. <https://doi.org/10.1016/j.dsr.2022.103735>
- Atmadipoera, A.S., Prartono, T., Jaya, I., Nugroho, D., Harsono, G., Nanlohy, P. & Koch-Larrouy, A., 2019. Seasonal variation of the upper-layer seawater properties in the Banda Sea: Observed from an autonomous CTD Argo float. *IOP Conf. Ser.: Earth Environ. Sci.*, 278(1): p.012008 <https://doi.org/10.1088/1755-1315/278/1/012008>

- Baeda, A.Y., Pao'Tonan, C. & Abdullah, D., 2019. The correlation between sea surface temperature and MJO incidence in Indonesian waters. *IOP Conf. Ser.: Earth Environ. Sci.*, 235(1): p.012020. <https://doi.org/10.1088/1755-1315/235/1/012020>
- Balaguru, K., Leung, L.R., Hagos, S.M. & Krishnakumar, S., 2021. An oceanic pathway for Madden-Julian Oscillation influence on Maritime Continent Tropical Cyclones. *npj Clim. Atmos. Sci.*, 4(1): p52. <https://doi.org/10.1038/s41612-021-00208-4>
- Barrett, B.S., 2019. Connections between the Madden-Julian Oscillation and surface temperatures in winter 2018 over eastern North America. *Atmos. Sci. Lett.*, 20(1): e.869. <https://doi.org/10.1002/asl.869>
- Barrett, B.S., Densmore, C.R., Ray, P. & Sanabia, E.R., 2021. Active and weakening MJO events in the Maritime Continent. *Clim. Dyn.*, 57: 157–172. <https://doi.org/10.1007/s00382-021-05699-8>
- Benthuisen, J.A., Oliver, E.C.J., Feng, M. & Marshall, A.G., 2018. Extreme Marine Warming Across Tropical Australia During Austral Summer 2015–2016. *J. Geophys. Res. Ocean.*, 123: 1301–1326. <https://doi.org/10.1002/2017JC013326>
- Chen, G. & Wang, B., 2020. Circulation factors determining the propagation speed of the Madden-Julian oscillation. *J. Clim.*, 33: 3367–3380. <https://doi.org/10.1175/JCLI-D-19-0661.1>
- de Boyer Montégut, C., Madec, G., Fischer, A.S., Lazar, A. & Iudicone, D., 2004. Mixed layer depth over the global ocean: An examination of profile data and a profile-based climatology. *J. Geophys. Res. Ocean.*, 109: 1–20. <https://doi.org/10.1029/2004JC002378>
- DeMott, C.A., Klingaman, N.P. & Woolnough, S.J., 2015. Atmosphere-ocean coupled processes in the Madden-Julian oscillation. *Rev. Geophys.*, 53(4): 1099-1154. <https://doi.org/10.1002/2014RG000478>
- Drushka, K., Sprintall, J., Gille, S.T. & Wijffels, S., 2012. In situ observations of Madden-Julian oscillation mixed layer dynamics in the Indian and western Pacific Oceans. *J. Clim.* 25: 2306–2328. <https://doi.org/10.1175/JCLI-D-11-00203.1>
- Feng, M., Duan, Y., Wijffels, S., Hsu, J.Y., Li, C., Wang, H., Yang, Y., Shen, H., Liu, J., Ning, C. & Yu, W., 2021. Tracking air-sea exchange and upper-ocean variability in the Indonesian-Australian basin during the onset of the 2018/19 Australian summer monsoon. *Bull. Am. Meteorol. Soc.*, 01(8): 1397-1412. <https://doi.org/10.1175/BAMS-D-19-0278.1>
- Habibullah, A.D. & Tarya, A., 2021. Sea surface temperature variability in Indonesia and its relation to regional climate indices. *IOP Conf. Ser.: Earth Environ. Sci.*, 925(1): p.012008. <https://doi.org/10.1088/1755-1315/925/1/012008>
- Hsu, J.Y., Feng, M. & Wijffels, S., 2022. Rapid restratification of the ocean surface boundary layer during the suppressed phase of the MJO in austral spring. *Environ. Res. Lett.*, 17(2): p.024031. <https://doi.org/10.1088/1748-9326/ac4f11>
- Huang, B., Liu, C., Banzon, V., Freeman, E., Graham, G., Hankins, B., Smith, T. & Zhang, H.M., 2021. Improvements of the Daily Optimum Interpolation Sea Surface Temperature (DOISST) Version 2.1. *J. Clim.*, 34: 2923–2939. <https://doi.org/10.1175/JCLI-D-20-0166.1>
- Huang, Z. & Feng, M., 2021. MJO induced diurnal sea surface temperature variations off the northwest shelf of Australia observed from Himawari geostationary satellite. *Deep. Res. Part II Top. Stud. Oceanogr.*, 183: p.104925. <https://doi.org/10.1016/j.dsr2.2021.104925>
- Jiang, X., Adames, Á.F., Kim, D., Maloney, E.D., Lin, H., Kim, H., Zhang, C., DeMott, C.A. & Klingaman, N.P., 2020. Fifty Years of Research on the Madden-Julian Oscillation: Recent Progress, Challenges, and Perspectives. *J. Geophys. Res. Atmos.*, 25(17), p.e2019JD030911. <https://doi.org/10.1029/2019JD030911>
- Kida, S. & Richards, K.J., 2009. Seasonal sea surface temperature variability in the Indonesian Seas. *J. Geophys. Res. Ocean.* 114(C6): C06016. <https://doi.org/10.1029/2008JC005150>
- Koch-Larrouy, A., Atmadipoera, A., van Beek, P., Madec, G., Aucan, J., Lyard, F., Grelet, J. & Souhaut, M., 2015. Estimates of tidal mixing in the Indonesian archipelago from multidisciplinary INDOMIX in-situ data. *Deep. Res. Part I Oceanogr. Res. Pap.*, 106: 136–153. <https://doi.org/10.1016/j.dsr.2015.09.007>
- Liang, Y., Du, Y., Zhang, L., Zheng, X. & Qiu, S., 2018. The 30-50-day intraseasonal oscillation of sst

- and precipitation in the South Tropical Indian Ocean. *Atmosphere*, 9(2): p.69. <https://doi.org/10.3390/atmos9020069>
- Lin, H., 2022. The Madden-Julian Oscillation. *Atmos - Ocean*, 60(3-4): 338-359 <https://doi.org/10.1080/07055900.2022.2072267>
- Liu, L., Li, Y. & Wang, F., 2021. MJO-Induced Intraseasonal Mixed Layer Depth Variability in the Equatorial Indian Ocean and Impacts on Subsurface Water Obduction. *J. Phys. Oceanogr.* 51: 1247-1263. <https://doi.org/10.1175/jpo-d-20-0179.1>
- Mao, J. & Wang, M., 2019. Intraseasonal responses of sea surface and deep oceanic temperature anomalies in the northern Indian Ocean-western Pacific to the 30-60-day boreal summer atmospheric intraseasonal oscillation. *Clim. Dyn.*, 53: 4539-4552. <https://doi.org/10.1007/s00382-019-04806-0>
- Matthews, A.J., Singhruck, P. & Heywood, K.J., 2010. Ocean temperature and salinity components of the Madden-Julian oscillation observed by Argo floats. *Clim. Dyn.*, 35: 1149-1168. <https://doi.org/10.1007/s00382-009-0631-7>
- Moteki, Q., Katsumata, M., Yoneyama, K., Ando, K. & Hasegawa, T., 2018. Drastic thickening of the barrier layer off the western coast of Sumatra due to the madden-julian oscillation passage during the pre-years of the maritime continent campaign. *Prog. Earth Planet. Sci.*, 5(1): 1-19. <https://doi.org/10.1186/s40645-018-0190-9>
- Napitu, A.M., Gordon, A.L. & Pujiana, K., 2015. Intraseasonal sea surface temperature variability across the Indonesian seas. *J. Clim.*, 28, 8710-8727. <https://doi.org/10.1175/JCLI-D-14-00758.1>
- Pei, S., Shinoda, T., Steffen, J. & Seo, H., 2021. Substantial Sea Surface Temperature Cooling in the Banda Sea Associated With the Madden-Julian Oscillation in the Boreal Winter of 2015. *J. Geophys. Res. Ocean.*, 126(6): p.e2021J C017226. <https://doi.org/10.1029/2021JC017226>
- Pujiana, K., Moum, J.N. & Smyth, W.D., 2018. The role of turbulence in redistributing upper-ocean heat, freshwater, and momentum in response to the MJO in the equatorial Indian Ocean. *J. Phys. Oceanogr.*, 48: 197-220. <https://doi.org/10.1175/JPO-D-17-0146.1>
- Purwandana, A., Cuypers, Y., Bouruet-Aubertot, P., Nagai, T., Hibiya, T. & Atmadipoera, A.S., 2020. Spatial structure of turbulent mixing inferred from historical CTD datasets in the Indonesian seas. *Prog. Oceanogr.*, 184: p.102312. <https://doi.org/10.1016/j.pocean.2020.102312>
- Sprintall, J., Gordon, A.L., Wijffels, S.E., Feng, M., Hu, S., Koch-Larrouy, A., Phillips, H., Nugroho, D., Napitu, A., Pujiana, K., Dwi Susanto, R., Sloyan, B., Yuan, D., Riama, N.F., Siswanto, S., Kuswardani, A., Arifin, Z., Wahyudi, A.J., Zhou, H., Nagai, T., Ansong, J.K., Bourdalle-Badié, R., Chanut, J., Lyard, F., Arbic, B.K., Ramdhani, A. & Setiawan, A., 2019. Detecting change in the Indonesian seas. *Front. Mar. Sci.*, 6: p.257 <https://doi.org/10.3389/fmars.2019.00257>
- Susanto, R.D. & Ray, R.D., 2022. Seasonal and Interannual Variability of Tidal Mixing Signatures in Indonesian Seas from High-Resolution Sea Surface Temperature. *Remote Sens.*, 14(8): p.1934. <https://doi.org/10.3390/rs14081934>
- Thomson, R.E. & Emery, W.J., 2014. Chapter 5 - Time Series Analysis Methods, in: Thomson, R.E., Emery, W.J. (Eds.), *Data Analysis Methods in Physical Oceanography* (Third Edition). Elsevier, Boston, pp. 425-591. <https://doi.org/10.1016/B978-0-12-387782-6.00005-3>
- Waliser, D., Sperber, K., Hendon, H., Kim, D., Maloney, E., Wheeler, M., Weickmann, K., Zhang, C., Donner, L., Gottschalck, J., Higgins, W., Kang, I.S., Legler, D., Moncrieff, M., Schubert, S., Stern, W., Vitart, F., Wang, B., Wang, W. & Woolnough, S., 2009. MJO simulation diagnostics. *J. Clim.*, 22: 3006-3030. <https://doi.org/10.1175/2008JCLI2731.1>
- Zhang, C., 2005. Madden-Julian Oscillation. *Rev. Geophys.* <https://doi.org/10.1029/2004RG000158>
- Zhang, C., Ling, J., 2017. Barrier effect of the Indo-Pacific Maritime Continent on the MJO: Perspectives from tracking MJO precipitation. *J. Clim.*, 30: 3439-3459. <https://doi.org/10.1175/JCLI-D-16-0614.1>